Available online at www.sciencedirect.com
ScienceDirect
Journal of Power Sources 170 (2007) 79–84
JOURNAL OF POWER SOURCES
www.elsevier.com/locate/jpowsour

Short communication

Carbon nanotube/polyaniline composite as anode material for microbial fuel cells

Yan Qiao [a,b], Chang Ming Li [a,b,*], Shu-Juan Bao [a,b], Qiao-Liang Bao [a,b]

[a] *School of Chemical and Biomedical Engineering, Nanyang Technological University, 70 Nanyang Drive, Singapore 637457, Singapore*
[b] *Center for Advanced Bionanosystems, Nanyang Technological University, 70 Nanyang Drive, Singapore 637457, Singapore*

Received 9 December 2006; accepted 7 March 2007
Available online 30 March 2007

Abstract

A carbon nanotube (CNT)/polyaniline (PANI) composite is evaluated as an anode material for high-power microbial fuel cells (MFCs). Fourier transform infrared spectroscopy (FTIR) and scanning electron microscopy (SEM) are employed to characterize the chemical composition and morphology of plain PANI and the CNT/PANI composite. The electrocatalytic behaviour of the composite anode is investigated by means of electrochemical impedance spectroscopy (EIS) and discharge experiments. The current generation profile and constant current discharge curves of anodes made from plain PANI, 1 wt.% and 20 wt.% CNT in CNT–PANI composites reveal that the performance of the composite anodes is superior. The 20 wt.% CNT composite anode has the highest electrochemical activity and its maximum power density is 42 mW m^{-2} with *Escherichia coli* as the microbial catalyst. In comparison with the reported performance of different anodes used in *E. coli*-based MFCs, the CNT/PANI composite anode is excellent and is promising for MFC applications.

Keywords: Polyaniline; Carbon nanotube; Microbial fuel cell; Anode modification; Power density

1. Introduction

Microbial fuel cells (MFCs) use bacteria as catalysts to oxidize organic and inorganic matter for energy generation. A number of factors affect MFC performance, namely, microbial inoculums, chemical substrate, proton exchange material (or absence of this material), cell internal and external resistance, solution ionic strength, electrode materials, and electrode spacing [1–3]. Among these factors, a high-performance electrode material is most essential. To improve the power output of MFCs, much research has focused on cathode modification and optimization of bacteria inoculums [4,5]. The anode is also an important determinant of MFC performance and is often the limiting factor for a high power output. The anode material and its structure can directly affect the bacteria attachment, electron transfer and substrate oxidation. To date, carbon materials such as carbon cloth and carbon paper are applied in most MFC anodes due to their stability in a microbial inoculum mixture, high conductivity and high specific surface-area. Nevertheless, they have little electrocatalytic activity for the anode microbial reactions and thus modification of the carbon materials is the main approach for improving their performance. Thus, there is a great need to develop a new type of anode material for MFCs that is more advantageous than regular carbon cloth and carbon papers.

Carbon nanotubes (CNTs) have exhibited very promising properties as a catalyst support in fuel cell applications due to their unique electrical and structural properties [6]. For example, CNTs are superior to carbon blacks as catalyst supports for proton exchange membrane fuel cells (PEMFCs) [7,8]. They have also served as anode materials for enzymatic biofuel cells [9,10]. It has been reported, however, that CNTs have a cellular toxicity that could lead to proliferation inhibition and cell death [11,12]. Thus, they are not suitable for MFCs unless modified to reduce the cellular toxicity.

Conductive polymers have attracted intensive research in different electrochemical devices [13–15]. Polyaniline (PANI) an important conducting polymer due to its relatively facile processability, electrical conductivity, and environmental stability.

* Corresponding author at: School of Chemical and Biomedical Engineering, Nanyang Technological University, 70 Nanyang Drive, Singapore 637457, Singapore. Tel.: +65 6790 4485; fax: +65 6791 1761.
E-mail address: ECMLi@ntu.edu.sg (C.M. Li).

0378-7753/$ – see front matter © 2007 Elsevier B.V. All rights reserved.
doi:10.1016/j.jpowsour.2007.03.048

The electronic properties of PANI can be reversibly controlled by both doping/de-doping and protonation processes, in which its emeralding base and emeraldine salt form can be interchanged [16]. The polymer has been used to detect microorganism such as *Escherichia coli* with an enzyme based method [17,18]. Schroder and Scholz [19] have employed PANI to modify a platinum electrode for use as the anode of MFC and obtained one order of magnitude increase in current outputs. Conductive PANI used in the MFC not only provides a protective function for bacteria, but also directly contributes to electrocatalysis to give a high current density [19,20]. On the other hand, the lower conductivity and poor electron transfer of PANI limit its application in MFCs.

The fabrication of CNT/PANI composites has attracted great interest in recent years because the incorporation of CNTs into PANI can result in new composite materials with enhanced electronic properties. For example, it has been reported [21] that PANI fibres containing CNTs displayed significant improvements in both mechanical strength and conductivity [21]. Liu et al. [22] constructed CNT/PANI multilayer films by means of a layer-by-layer assembly method, and the CNTs inside the multilayer film could expand the electroactivity of PANI to a neutral electrolyte. Thus, the enhanced conductive CNT/PANI composite could possibly be used in MFCs for performance improvement. The electrocatalytic behaviour and application of the CNT/PANI composite in MFCs has not been studied. In the work reported here, a CNT/PANI composite is used as an anode of MFCs and its electrocatalytic properties associated with a bacterium biocatalyst are examined.

2. Experimental

2.1. Chemicals and materials

Aniline (≥99.0%), ammonium persulfate (APS, ACS reagent, ≥98.0%), polytetrafluoroethylene (PTFE) solution (1 wt.%) and 2-hydrox-1,4-naphthoquinone (HNQ, 97%) were obtained from Sigma–Aldrich. Multi-walled CNTs (95%, 10–20 nm) were received from Shenzhen Nanotech Co. Ltd. (Shenzhen, China). All other chemicals were of analytical grade and used as-received, unless stated otherwise. De-ionized (DI) water (resistance over 18 MΩ cm) from a Millipore Q water purification system was used in all experiments.

2.2. Synthesis of PANI and CNT/PANI composites

Aniline monomer was distilled under reduced pressure before polymerization. The PANI was chemically synthesized as follows: aniline (1 mL) was mixed with HCl (0.3 mL) in 50 mL DI water in an ice bath. An APS solution (2.3 g in 25 mL DI water) was added to the mixture. The polymerization was carried out for 6 h in the ice bath (0–5 °C). A green solid of proton-doped PANI was obtained after rinsing with DI water for several times. The CNTs were ultrasonically treated using a mixture of 3:1 of H_2SO_4:HNO_3 at 50 °C for 24 h to produce carboxylic acid groups at the defect sites and thereby improve solubility in HCl solution. The composite of proton-doped PANI/CNT was synthesized *in situ* via chemical oxidation. Different weight ratios of CNT to aniline were used. The CNTs were dissolved in 1.0 M HCl solution, subjected to ultrasonic treatment for 3 h, and then transferred to a 250 mL flask placed in the ice bath. A 1.0 M HCl aniline monomer solution was added to the prepared CNT–HCl suspension. The APS solution was added to the suspension with constant stirring at 0–5 °C for 6 h. A precipitate was produced. After filtering and rinsing for several times with DI water and methanol, the precipitate was vacuum-dried at 60 °C for 24 h and a powder containing CNT and PANI was obtained, which was ready for preparation of the anode of the MFC.

2.3. Characterization of PANI and CNT/PANI composite

Infrared spectra were obtained by means of Fourier transform infrared spectroscopy (Nicolet MAGNA-IR 560, FTIR, U.S.A.) with an attenuated total reflection (ATR) accessory. The morphology of the plain PANI and the CNT/PANI composite powder was studied with a JEOL 6700 field emission scanning electron microscope (FESEM). Nitrogen adsorption isotherms were measured with an automated gas sorption system (AUTOSORB-1, Quantachrome Instruments) at liquid nitrogen temperature. The specific surface-area was calculated using Brunauer–Emmett–Teller (BET) method.

2.4. Electrode preparation

The plain PANI and its composite powders were mixed with a PTFE solution to prepare pastes. The pastes were coated on the surface of nickel foams (1 cm × 1 cm × 0.1 cm) to produce uniform films that were then pressed to fabricate PANI and CNT/PANI electrodes, respectively. The film covered the whole surface of the foam to prevent exposure of the nickel to the electrolyte. After drying at 120 °C to remove water, the electrodes were used as anodes for MFCs.

2.5. Bacteria growth

E. coli K12 (ATCC 29181) was grown anaerobically at 37 °C for 12 h in a standard glucose medium, which was a mixture of 10 g glucose, 5 g yeast extract, 10 g $NaHCO_3$ and 8.5 g NaH_2PO_4 per litre. For chronoamperometric measurements, the overnight culture in the above medium was inoculated into a fresh anaerobic medium. For impedance and constant-current discharge experiments, bacteria culture was harvested by centrifuging at 4 °C (6000 rpm, 5 min). The produced bacteria were washed for three times and then suspended in a 0.1 M anaerobic phosphate buffer containing 5.5 mM glucose. The concentration of *E. coli* cells was about 10^9 cells mL^{-1}. Before every test, nitrogen was purged into the suspension for 20 min to remove oxygen from the cell.

2.6. Electrochemical measurements

All electrochemical experiments were carried out with PGSTAT30 Autolab system (Ecochemie, Netherlands) in a three-electrode cell that consisted of the working electrode, a

saturated calomel (sat. KCl) reference electrode, and a platinum wire counter electrode. 2-Hydroxy-1,4-naphthoquinone (HNQ) was chosen as the electron mediator because it can generate higher coulombic output than commonly used mediators such as resazurin or thionine [23]. Except otherwise stated, electrochemical impedance measurements for the PNAI and CNT/PANI composite electrodes were performed over a frequency range of 0.5 Hz to 100 KHz in 0.1 M phosphate buffer at open-circuit potential and a perturbation signal of 10 mV.

3. Results and discussion

3.1. FTIR spectroscopy and morphology characterization

The FTIR spectra of plain PANI and the CNT/PANI composite are shown in Fig. 1. The peak at 835 cm^{-1} is attributed to the N–H out-of-plane bending absorption. The peaks at 1500 and 1600 cm^{-1} can be assigned to the stretching vibration of the quinoid ring and benzenoid ring, respectively, which are characteristic of PANI. The presence and the enhanced relative intensity of the absorption band with a maximum at 1240 cm^{-1} for the composites are very prominent. The features are due to the C–N stretching vibration in proton-doped PANI. The fact of the remarkable enhancement of the spectra indicates the formation of C–N coordinate-covalent bonds between the polymer chain and the radical cation CNT fragments [16,24]. The broad band at 1730 cm^{-1} in PANI (C=O vibration) is drastically enhanced for the CNT/PANI composite and becomes the most prominent peak for the 20 wt.% CNT/PANI powder. The band near 3000 cm^{-1} is due to the C–H stretching absorption. This signal is broad and strong in the composite samples and relatively weak in the plain PANI. This phenomenon was reported recently and it was explained that the sp^2 carbons of the carbon nanotubes perturbed the H-bonding environment and then increased the N–H stretch intensity. These results strongly support the formation of CNT/PANI through the chemical oxidation method.

Scanning electron micrographs of films made from plain PANI and the CNT/PANI composite powders are shown in Fig. 2. The pure PANI film is compact and fibrillar, while the CNT/PANI composite films have a networked-rod nanostructure, in which the outer layer is PANI and the inner layer is constructed by CNTs. The rough, amorphous outer PANI layer has an average thickness of about several tens of nanometers. To verify the effect of CNT doping on the structure of the polymer, the specific surface-areas of plain PANI and the nanocomposite were measured. The cumulative adsorption surface area (BJH Method) of plain PANI is 34.1 $m^2\ g^{-1}$. For the nanocomposite, the value is 50.2 $m^2\ g^{-1}$. These values show that the specific surface-area of the composite is much larger than that of the plain polymer. Therefore, it is expected that the difference in the structure of the materials can result in different discharge profiles and impedance spectra of the anodes constructed from these materials.

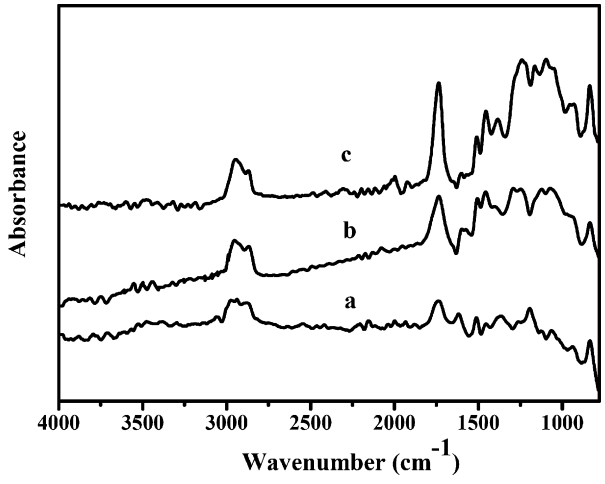

Fig. 1. FTIR spectra of PANI and composite powders (a: plain PANI; b: 1 wt.% CNT/PANI composite; c: 20 wt.% CNT/PANI composite).

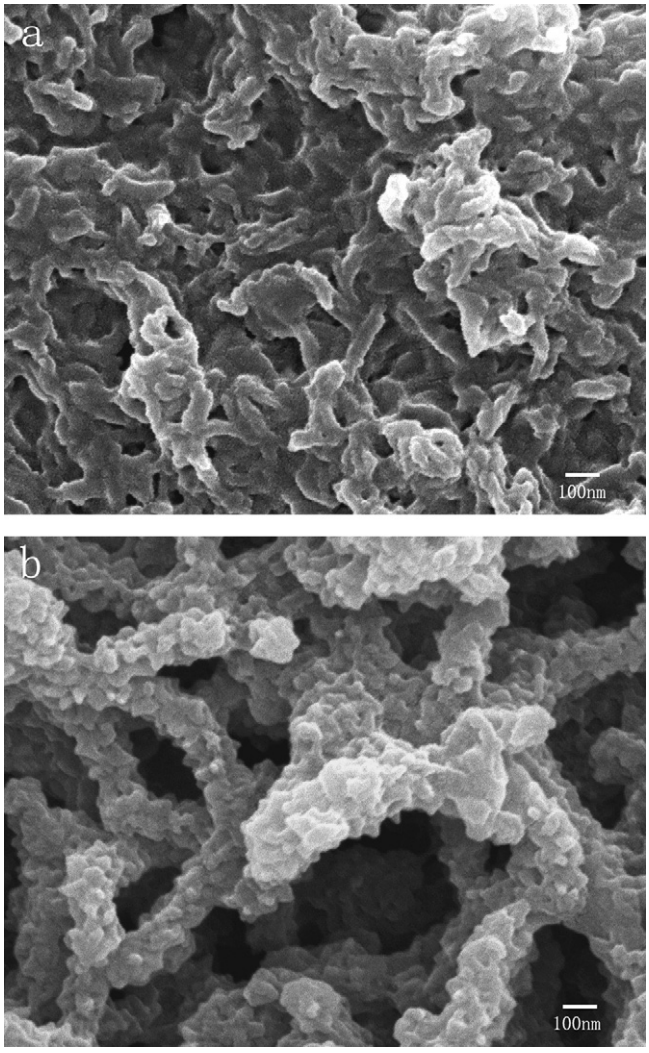

Fig. 2. SEM images of PANI and CNT/PANI composite films (a: plain PANI; b: 20 wt.% CNT/PANI composite).

3.2. Electrochemical impedance spectra studies

Electrochemical impedance spectroscopy (EIS) measurements were carried out to compare the characteristics of charge

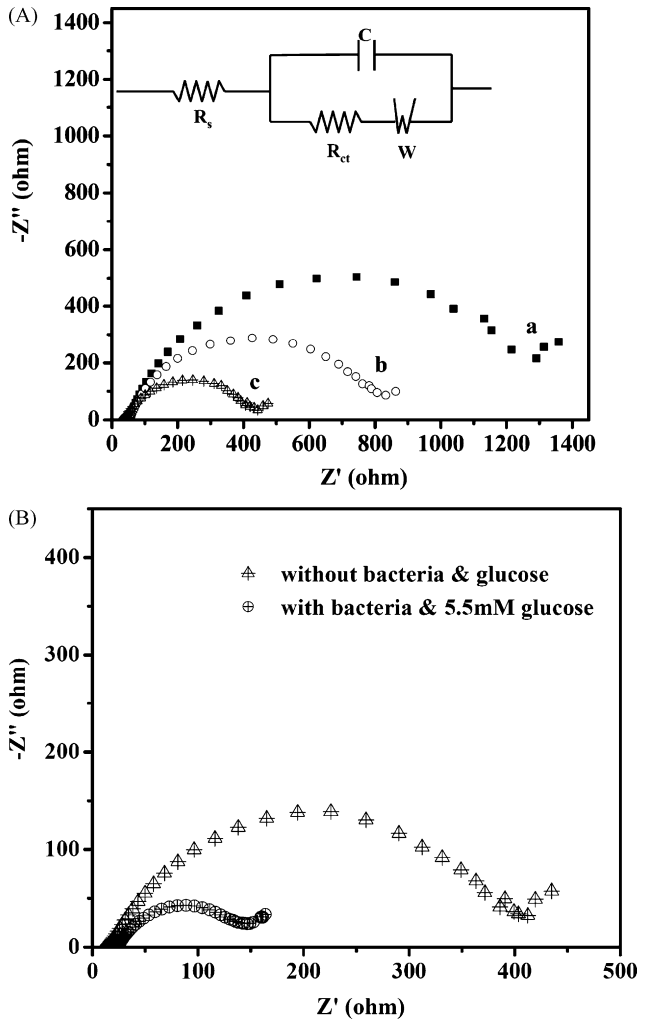

Fig. 3. (A) EIS of PANI (a), 1 wt.% CNT/PANI (b) and 20 wt.% CNT/PANI (c) composite electrode in 0.1 M phosphate buffer (pH 7) at open-circuit potential and equivalent circuit used to fit the EIS. (B) EIS of 20 wt.% CNT/PANI in 0.1 M phosphate buffer with or without bacteria and glucose at 100 mV vs. SCE.

transfer and ion transport in plain and composite polymers. The measured EIS results (Fig. 3) show well-defined single semicircles over the high frequency range, followed by short straight lines in the low-frequency region for all samples. Although the impedance spectra have similar shapes, the diameters of the semicircles decline greatly with increasing content of the CNTs in the polymer film. The diameter of the semicircle corresponds to the interfacial charge-transfer resistance (R_{ct}), which usually represents the resistance of electrochemical reactions on the electrode and is often called the Faraday resistance [25]. In the absence of bacteria and glucose, the R_{ct} of the three electrodes is 1317 (PANI), 827 (1 wt.% CNT/PANI) and 434 Ω (20 wt.% CNT/PANI), respectively. Obviously, the R_{ct} of the CNT/PANI composite is much lower than that of the pure polyaniline. Since there are no glucose and bacteria in the electrolyte, the R_{ct} should be ascribed to the doping/de-doping redox reactions of PANI. The impedance plane plots in Fig. 3 show only a very short part of a straight line region, which is an indication of diffusion control for the doping/de-doping process [25]. It is known that the reactants in the doping/de-doping reaction are anions. The narrow region of the diffusion-controlled process indicates that all the tested anodes have a good micro/nanostructure for the reactant to access the reaction centres without a diffusion limit over a wide frequency range. In a conducting polymer/CNT composite, it has been suggested that either the polymer functionalizes the CNTs, or the conductive polymer is doped with CNTs, and a charge transfer occurs between the two constituents [26]. It is also considered that the CNTs have an obvious improvement effect for a faster charge transfer rate than with plain PANI. The EIS of the 20 wt.% CNT/PANI electrode in phosphate buffer in the presence of bacteria with and without 5.5 mM glucose were also investigated at a dc bias of 100 mV versus SCE. The results are shown in Fig. 3B. When the electrode is tested in the phosphate buffer with both bacteria and glucose, the R_{ct} is about 156 Ω, which is significantly smaller than that in presence of bacteria but without glucose in the electrolyte (400 Ω). As discussed above, the electrochemical reactions without glucose in the solution are due to the doping/de-doping process of PANI. The significant reduction in R_{ct} indicates that the glucose oxidation in such a CNT/PANI/HNQ/*E. coli K12* anode system has an even faster reaction rate than that of the doping/de-doping redox reaction. The result reveals that the composite anode not only improves the electrode conductivity and specific surface-area, but also provides unique active centres, possibly due to its specific nanostructure as shown in Fig. 2b, to host the bacteria for more efficient electrocatalysis.

3.3. Anode discharge performance in MFC

In order to evaluate the discharge performance of different anodes in a MFC, an anode-limiting MFC was designed which had a Pt cathode with a much larger surface area than that of the anodes. Thus, polarization of the cathode was insignificant. The catalytic current from glucose oxidation at a constant potential was measured. As shown in Fig. 4, the current increases with the

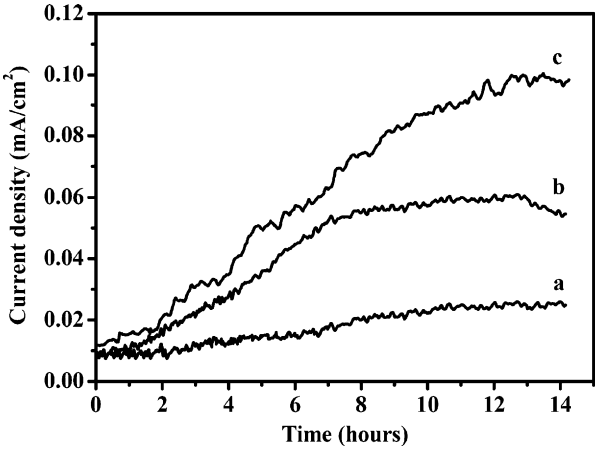

Fig. 4. Chronoamperometric plots of PANI and CNT/PANI composite electrodes placed in stirred anaerobic culture of *Escherichia coli* K12 in standard glucose medium. Potential applied to electrode is 0.1 V. Curve a: plain PANI; b: CNT/PANI composite containing 1 wt.% CNT; c: CNT/PANI composite containing 20 wt.% CNT.

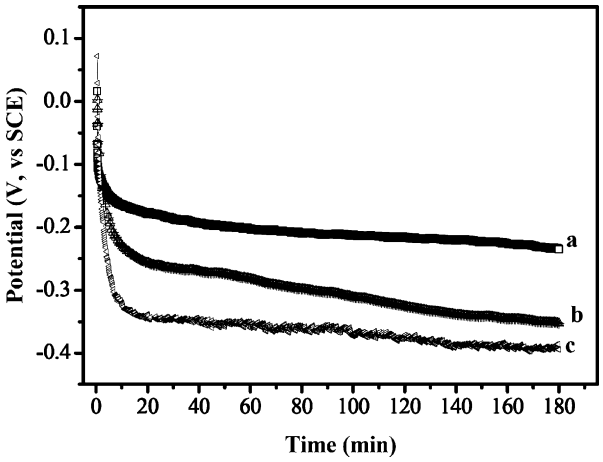

Fig. 5. Potential–time curve of PANI and CNT/PANI composite electrodes placed in a stirred anaerobic culture of *E. coli* K12 in 0.1 M phosphate buffer with 5.5 mM glucose. Curve a: plain PANI; b: CNT/PANI composite containing 1 wt.% CNT; c: CNT/PANI composite containing 20 wt.% CNT.

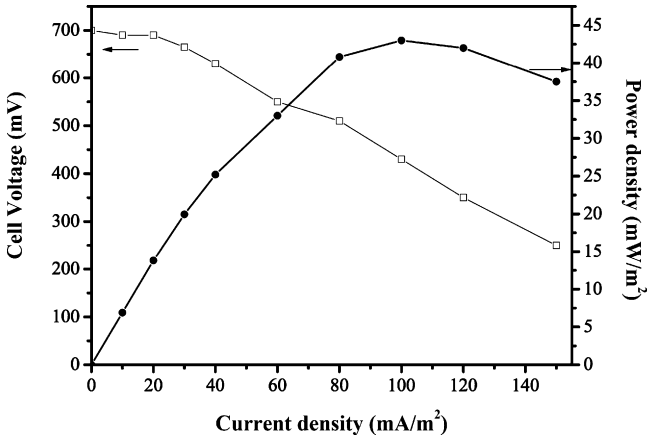

Fig. 6. Power output and polarization curve of MFC with 20 wt.% CNT/PANI anode.

growth and proliferation of the bacteria on the electrode surface. The current–time curves of PANI and composite anodes are significantly different from each other. For the plain PANI anode, the current increases very slowly and the current density is much lower than that the composites. For the two CNT/PANI composite anodes, when the current of the 1 wt.% CNT/PANI anode reaches a plateau, the current of the 20 wt.% CNT/PANI anode is still increasing and the current density is much higher than the former. This can be explained by the fact that the nanocomposite electrodes have more reaction activity sites (larger specific surface-area) for the bacteria-catalytic oxidation of glucose and the active sites increase with increasing doping of the CNTs. This result is in agreement with the impedance analysis and the BET results.

The constant-current discharge experiments of the MFCs with three different anodes in 5.5 mM glucose solution were conducted at 50 mA m^{-2}. The anode potential versus time data (Fig. 5) show different discharge profiles for the three anodes. Within 180 min, the discharge potentials for plain PANI, 1 wt.% CNT/PANI and 20 wt.% CNT/PANI change from −0.01 to −0.2, −0.36, and −0.38 V, respectively. For a fuel cell system, the more negative the anode discharge potential, the higher is the operational voltage of the fuel cell. The discharge results show that the composite anode can provide a higher power density due to its lower polarization, which further indicates that the nanostructured composites have a faster reaction rate. It is also seen that the composite with the higher CNT content (20 wt.%) gives a better discharge performance than that with a lower CNT content (1 wt.%). It is observed that the discharge profile of the bacteria anode is fundamentally different from that of conventional anode behaviour. The bacteria anode has a high polarization potential initially and thus becomes lower with the extension of the discharge time. This is due to the bacteria growth process since the discharge process starts immediately after addition of glucose solution and bacteria. The bacteria require time to grow to their maximum level and to distribute into the inner surface of the anode, as shown in Fig. 4.

3.4. Power output of 20 wt.% CNT/PANI MFC

As the 20 wt.% CNT/PANI MFC exhibits the best performance, its power output and polarization was examined with the anode-limiting MFC. The results are presented in Fig. 6. The polarization curve shows that the cell voltage drops to 250 mV at a current density of 145 mA m^{-2}. The power density of the 20 wt.% CNT/PANI MFC is calculated from the results of chronopotential measurements under different current densities. The plot of power density versus current density has a volcano shape. The power density increases with increase in current density, reaches a maximum value, and then sharply falls with further increase in current density. This is a typical relationship of output power density against the current density. The maximum power density is 42 mW m^{-2}, which is obtained at a current density of about 100 mA m^{-2} with a cell voltage of 450 mV. It has been reported [27] that woven graphite electrodes in *E. coli* microbial fuel cells could deliver a maximum power density of 0.47–2.6 mW m^{-2} with cell voltages of 0.6–3.3 V; the power density reached 91 mW m^{-2} with Mn^{4+} modified woven graphite as the anode but the cell voltage was about 0.28 V. Given that the thickness of the anode used in our work is smaller than 1 mm in comparison with the 1 cm thickness of the anodes used in [27], the CNT/PANI anode has superior electrocatalytic activity.

4. Conclusions

This study has shown that a nanostructured CNT/PANI nanocomposite can be used as the anode for a microbial fuel cell. The addition of CNTs to PANI increases the specific surface-area of the electrode and enhances the charge transfer capability so as to cause considerable improvement of the electrochemical activity for the anode reaction in a MFC. A CNT/PANI/*E. coli* K12/HNQ anode system gives a much higher power output than that of a PANI/*E. coli* K12/HNQ system. This demonstrates the superior and specific electrocatalytic effect of the nanocomposite for MFCs in comparison the existing systems. The composite containing 20 wt.% CNT gives the best discharge performance and delivers a high power output of 42 mW m^{-2} with a cell volt-

age of 450 mV. The CNT-doped PANI nanocomposite therefore offers good prospects for application in MFCs.

Acknowledgement

The authors are grateful to the Asian Office of Aerospace Research and Development, Department of The Air Force of USA, for financial support under contract of AOARD-05-4073.

References

[1] B.E. Logan, B. Hamelers, R. Rozendal, et al., Environ. Sci. Technol. 40 (2006) 5181–5192.
[2] R.A. Bullen, T.C. Arnot, J.B. Lakeman, et al., Biosens. Bioelectron. 21 (2006) 2015–2045.
[3] K. Rabaey, W. Verstraete, Trends Biotechnol. 23 (2005) 291–298.
[4] R.M. Allen, H.P. Bennetto, Appl. Biochem. Biotechnol. 39 (1993) 27–40.
[5] S.K. Chaudhuri, D.R. Lovley, Nat. Biotechnol. 21 (2003) 1229–1232.
[6] H.S. Liu, C.J. Song, L. Zhang, et al., J. Power Sources 155 (2006) 95–110.
[7] Z.L. Liu, X.H. Lin, J.Y. Lee, et al., Langmuir 18 (2002) 4054–4060.
[8] C. Wang, M. Waje, X. Wang, et al., Nano Letters 4 (2004) 345–348.
[9] D. Ivnitski, B. Branch, P. Atanassov, et al., Electrochem. Commun. 8 (2006) 1204–1210.
[10] Y.M. Yan, W. Zheng, L. Su, et al., Adv. Mater. 18 (2006) 2639.
[11] E. Flahaut, M.C. Durrieu, M. Remy-Zolghadri, et al., J. Mater. Sci. 41 (2006) 2411–2416.
[12] A. Magrez, S. Kasas, V. Salicio, et al., Nano Letters 6 (2006) 1121–1125.
[13] T.A.R.L.E. Skotheim, J.R. Reynolds, Handbook of Conducting Polymers, Dekker, New York, 1998.
[14] C.M. Li, W. Chen, X. Yang, et al., Front. Biosci. 10 (2005) 2518–2526.
[15] H. Dong, C.M. Li, W. Chen, et al., Anal. Chem. 8 (2006) 7424–7431.
[16] W.Z. Huseyin Zengin, J. Jin, R. Czerw, D.W. Smith Jr., L. Echegoyen, D.L. Carroll, S.H. Foulger, J. Ballato, Adv. Mater. 14 (2002) 1480–1483.
[17] Z. Muhammad-Tahir, E.C. Alocilja, IEEE Sens. J. 3 (2003) 345–351.
[18] S.C.K. Misra, R. Angelucci, Indian J. Pure Appl. Phys. 39 (2001) 726–730.
[19] J.N. Uwe Schroder, F. Scholz, Angewandte Chemie 115 (2003) 2986–2989.
[20] U.S. Juliane Niessen, M. Rosenbaum, F. Scholz, Electrochem. Commun. 6 (2004) 571–575.
[21] V. Mottaghitalab, G.M. Spinks, G.G. Wallace, Synth. Met. 152 (2005) 77–80.
[22] J.Y. Liu, S.J. Tian, W. Knoll, Langmuir 21 (2005) 5596–5599.
[23] S.A. Lee, Y. Choi, S.H. Jung, et al., Bioelectrochemistry 57 (2002) 173–178.
[24] A.M.B. Raquel Sainz, M. Teresa Martinez, J.F. Galindo, J. Sotres, A.M. Baro, B. Corraze, O. Chauvet, W.K. Master, Adv. Mater. 17 (2005) 278–281.
[25] A.J. Bard, L.R. Faulkner, Electrochemical Methods: Fundamentals and Applications, 2nd ed., Wiley, New York, 2001.
[26] D.J. Guo, H.L. Li, J. Solid State Electrochem. 9 (2005) 445–449.
[27] D.H. Park, J.G. Zeikus, Biotechnol. Bioeng. 81 (2003) 348–355.